1998-06

# Sulphur hexafluoride as a tracer of biogeochemical and physical processes in an open-ocean iron fertilisation experiment

Law, C.S; Watson, A.J; Liddicoat, M.I; Stanton, T.

Pergamon

Law, C. S., et al. "Sulphur hexafluoride as a tracer of biogeochemical and physical processes in an open-ocean iron fertilisation experiment." Deep Sea Research Part II: Topical Studies in Oceanography 45.6 (1998): 977-994.
http://hdl.handle.net/10945/62335

PERGAMON

Deep-Sea Research II 45 (1998) 977–994

DEEP-SEA RESEARCH
PART II

# Sulphur hexafluoride as a tracer of biogeochemical and physical processes in an open-ocean iron fertilisation experiment

C.S. Law[a,*], A.J. Watson[a,†], M.I. Liddicoat[a], T. Stanton[b]

[a] *Plymouth Marine Laboratory, Prospect Place, West Hoe, Plymouth, Devon PL1 3DH, UK*
[b] *Naval Postgraduate School, Monterey, CA 93943-5000, USA*

Received 1 November 1995; received in revised form 20 April 1997; accepted 20 April 1997

**Abstract**

The first open-ocean experiment to test the iron hypothesis in the equatorial Pacific was undertaken using the tracer gas sulphur hexafluoride ($SF_6$) to locate and track the fertilised surface water. Continuous surface measurements showed that the $SF_6$ patch spread rapidly in the first 24 h, from an initial release area of $\sim 64\,km^2$ to a total area of $214\,km^2$, and remained relatively constant in size for the following three-day period. $SF_6$ data was mapped in a Lagrangian frame of reference by the use of a drogued GPS buoy released at the centre of the patch. The $SF_6$ patch remained coherent and exhibited a slow, anti-cyclonic oscillation during the first four days. The buoy was transported downwind of the patch in a north-westerly direction within two days, which has implications for the future use of buoys in surface-water advection studies. Following subduction below a low-salinity front 3–4 days after release, the patch centre was relocated by its $SF_6$ signal at a depth of 25–30 m to the east of the residual surface patch. The latter spread rapidly to the southwest during the remainder of the experiment, whilst the subducted patch remained relatively stationary. Density-corrected $SF_6$ profiles were used to calculate a mean vertical eddy diffusivity of $0.25\,cm^2/s$ across the thermocline following the subduction event. A vertical flux of nitrate of $2.5\,mmol/m^{-2}d^{-1}$ into the mixed layer was estimated, which implied an *f*-ratio value of 0.4 on comparison with productivity data. The results demonstrate that $SF_6$ is a successful tracer of water masses, and emphasise the potential of this technique for the *in situ* measurement and manipulation of open-ocean processes. 

* Corresponding author. E-mail: C.law@pml.ac.uk; Fax: 0044 1752 633101.
† Now at: School of Environmental Science, University of East Anglia, Norwich NR4 7TJ, UK.

0967-0645/98/$–see front matter 
PII: S0967-0645(98)00022-8

## 1. Introduction

Direct measurement of the physical characteristics of the marine environment by the tracking of water bodies and delineation of flow rates has been achieved through a variety of methods. The use of floats has been extensively modified to the point where satellite communication facilitates location of their exact position in near-real time, although surface buoys tend to experience wind-slippage to some extent (Pingree, 1989). Surface-water flow also may be monitored by the use of suspended or dissolved substances, including naturally occurring tracers, passive anthropogenic substances such as radiogenic compounds and fluorocarbons, and applied tracers such as the dyes rhodamine and fluorocin (Smart and Laidlow, 1977). Analytical systems with suitable sensitivity limits are available for tracking the latter species during dispersion and dilution of a water body, but dyes are non-conservative and relatively toxic to handlers and the environment, as well as expensive. The use of the man-made gas sulphur hexafluoride ($SF_6$) as a tracer overcomes these problems, as demonstrated by recent surface and deep water releases studying air–sea exchange and vertical and lateral diffusivity rates (Watson et al., 1991; Wanninkhof et al., 1993; Ledwell et al., 1993). Analytical detection limits at the sub-femtomolar range (1 fmol $= 10^{-15}$ mol) and an extremely low surface water background concentration of $<1.2$ fmol/l permit macroscale water mass tracking with modest releases of $SF_6$ (Ledwell et al., 1993). This combined with the automation of discrete and continuous analytical systems with short analysis times (Upstill-Goddard et al., 1991; Law et al., 1994) facilitates the collection of large, accurate data sets. Although non-toxic, $SF_6$ is a potent greenhouse gas as a result of its long atmospheric lifetime, but the quantities required for a tracer release experiment are small compared to global emissions, with a surface release accounting for less than $10^{-6}$ of the annual global production rate (Ko et al., 1993). A minor disadvantage in the use of $SF_6$ as a tracer is its volatility, which reduces the time frame within which a surface release can be followed. The loss rate of $SF_6$ across the air–sea interface is well-documented (Watson et al., 1991; Wanninkhof, 1992), and so readily quantified, and so the volume of tracer required for a release can be calculated in advance.

The application of $SF_6$ as a tracer is not restricted to physical measurements. Tagging with $SF_6$ also facilitates the measurement of temporal change in the biology and biogeochemistry of a discrete body of water. This labelling also permits the manipulation of the water body in question, and so removes the restrictions and limitations of marine experimentation at the laboratory level. Iron limitation of primary productivity has been clearly demonstrated in *in vitro* studies (Martin et al., 1988, 1990), but the relevance of these results to the open ocean has been questioned due to the exclusion of factors such as zooplankton grazing and mixing (Banse, 1990). To address these shortcomings, a combined mesoscale release of iron and $SF_6$ into surface waters was suggested (Watson et al., 1991), so that the iron-enriched waters, and resultant changes in the biological and biogeochemical signal, could be followed regardless of the influence of surface hydrodynamics. The $SF_6$ would additionally function as a surrogate for the iron, so that the ecosystem response could still be determined when concentrations had fallen below detection limits. The following

paper describes the results of the deployment of $SF_6$ as a tracer in the first open-ocean iron fertilisation experiment (IRONEX) at 5°S 90°W in the Equatorial South Pacific (Martin et al., 1994; Watson et al., 1994). Dispersion of the patch, which subducted to a depth of 25–30 m after 3–4 days, is described and budgeted. In addition, the vertical diffusion rate across the thermocline is estimated from the $SF_6$ distribution, and applied to the nitrate distribution to obtain an estimate of the contribution to new production.

## 2. Methods

### 2.1. Tracer preparation and release

The saturated $SF_6$ solution was prepared in the University of Miami boatyard prior to sailing, following the methods described by Upstill-Goddard et al. (1991). A 2250 l steel tank was filled with freshwater with salinity corrected to approximately 35‰ by addition of sodium chloride to minimise density differences upon tracer release. A perspex cylinder bolted to the top of the tank and sealed with an air-tight gasket provided a headspace of approximately 5 l, with the upper lid of the cylinder housing five Swagelok bulkhead unions which facilitated gas circulation via 1/8″ stainless steel and copper tubing. The headspace was flushed with pure $SF_6$ at a rate of 120 ml $min^{-1}$, with concurrent circulation of the headspace gas through the water via a series of airstones suspended in the base of the tank and a Compton air pump. Saturation was monitored at regular intervals by headspace equilibrium between a 50 ml subsample of the water and 50 ml of oxygen-free nitrogen in a syringe. Two ml of the headspace were subsequently injected onto a 3 m 1/8″ Porapak QS/Molecular Sieve 5A column with detection by Thermal Conductivity Dectector-Gas Chromatography (Shimadzu TCD GC-8AIT). Rate of saturation and TCD performance were established by comparison with a 0.18% $SF_6$ standard. $SF_6$ saturation in the tank was checked prior to and during the release confirming that no significant loss of $SF_6$ had occurred.

The concurrent release of the tracer and iron solution has been described by Fitzwater et al. (1994). The tracer was pumped from the saturation tank at a rate of 1.4 l/min with the displaced volume being replaced by gravity by filling a weather balloon within the tank with water. This method avoided dilution of the tracer and exposure of the tank contents to the air, and so prevented degassing. After mixing with the iron solution, the tracer was released through two pipes directly aft of the propellers whilst the ship was travelling at 9 km/h for a period of approximately 23.5 h from 2000 GMT on Julian Day 297 (JD297 – 24/10/93). A GPS buoy, attached to a "holey-sock" drogue to reduce wind slippage, was released at the centre of the patch for location and provision of a Lagrangian frame of reference (Stanton et al., this volume).

### 2.2. $SF_6$ analysis

Continuous sampling of the surface water began at 2000 GMT on JD298, using a sparge and cryogenic trap system as described in Upstill-Goddard et al. (1991) with

modifications. Surface water was transported to the analytical system in the laboratory via the ships non-toxic system, which had an inlet depth of 3 m and minimal residence time. Two peristaltic pumps (Watson-Marlow) maintained inlet and outlet water flow to a glass sparge tower at a constant rate of 80 ml/min. Flow rate was also regulated by a two-way solenoid valve on the inlet that was activated and deactivated by feedback from a level sensor incorporated in the sparge tower. A second sensor-solenoid system was also incorporated to prevent flooding in the event of primary sensor failure. Oxygen-free nitrogen stripped the $SF_6$ from solution and transported it through a drier to a Porapak QS trap suspended in a propanol bath at a temperature of $-70°C$. At 3 min intervals the sparge flow was diverted to a second cryogenically cooled trap, and the first trap was raised out of the propanol and heated rapidly to 70°C. Carrier flow transported the $SF_6$ from the trap onto a 2 m Molecular Sieve 5A column with subsequent $SF_6$ detection by Electron Capture Detector (Shimadzu GC-8AIE). The ships sampling speed was $\sim 5$ knots (9.3 km/h) between JD298 and JD301, resulting in a measurement every 0.45 km of the ships track. Results were immediately incorporated into a near real-time plot of relative positions of the patch centre and ship, by integrating the $SF_6$ data with the ships GPS position. This enabled rapid alterations to the ships speed and direction in response to a change in the $SF_6$ signal and ensured adequate coverage of the patch, as well as determining the positions of the "IN" and "OUT" patch sampling stations.

Discrete samples were collected via CTD hydrocasts to determine the vertical structure of the patch, and for comparison with the distribution of other variables including carbon dioxide (Watson et al., 1994) and dimethylated sulphur compounds (Turner et al., 1996). BOD bottles were filled directly from the CTD Niskins and overflowed by at least 100% to negate $SF_6$ loss to the atmosphere. Samples were analysed immediately using a dedicated system based on the same principles as the continuous system, but incorporating a vacuum-sparge system for rapid extraction, as described in Law et al. (1994). The sample was drawn into an evacuated glass sparge tower and stripped by oxygen-free nitrogen. Initial patch samples were analysed using a tower volume of 50 ml, whilst background samples, e.g., pre-release and "OUT" stations were analysed using a 350 ml sparge tower. Trapping and analysis were as described above with the exception that only one trap was used in the discrete system.

Calibration of both systems was achieved using a set of five $SF_6$ in nitrogen standards prepared at Plymouth Marine Laboratory in the range 10.4 pptv–3 ppbv (Law et al., 1994). The discrete system was calibrated at approximately 24 h intervals, whereas the continuous system, which played a more qualitative role, was calibrated at the start and end of the experiment. Detection limits were 0.03 and 0.07 fmol/l for the discrete and continuous systems, respectively, with $\sim 6000$ samples analysed by the continuous system and $\sim 1000$ by the discrete system. Reproducibility of duplicate and triplicate sample analysis on the discrete system was 0.77% for tracer samples and 1.4% for pre-release background samples. Regular comparison between the two systems showed that the stripping efficiency of the continuous system was always $>97\%$. Minor routine maintenance to the continuous system, including desiccant and peristaltic pump tube replacement and data downloading, had little

effect on coverage of the patch, with the system operational for 96% of the duration of the experiment.

## 3. Results and discussion

### 3.1. Background $SF_6$

The presence of $SF_6$ in the atmosphere ($\sim$3 pptv) produces a background concentration in the upper water column as a result of air–sea exchange, although this is extremely small due to the low solubility of the gas. Six pre-release casts were initially undertaken to determine the uniformity of the region initially assigned for the tracer release (Fig. 1a). As the atmosphere represents the sole source, $SF_6$ concentrations were highest at the surface ($0.548 \pm 0.014$ fmol/l), and remained constant in the mixed layer ($0.544 \pm 0.014$ fmol/l) (Fig. 1b). These data have since been incorporated with atmospheric and surface water data from other regions to derive an atmospheric history for $SF_6$ (Law et al., 1994), which compares favourably with other contemporaneous chronologies (Maiss et al., 1994, 1996). The role of the pycnocline as a barrier to vertical exchange was apparent from the sharp decline in $SF_6$ at approximately 35–40 m, below which concentration gradually decreased to approximately three

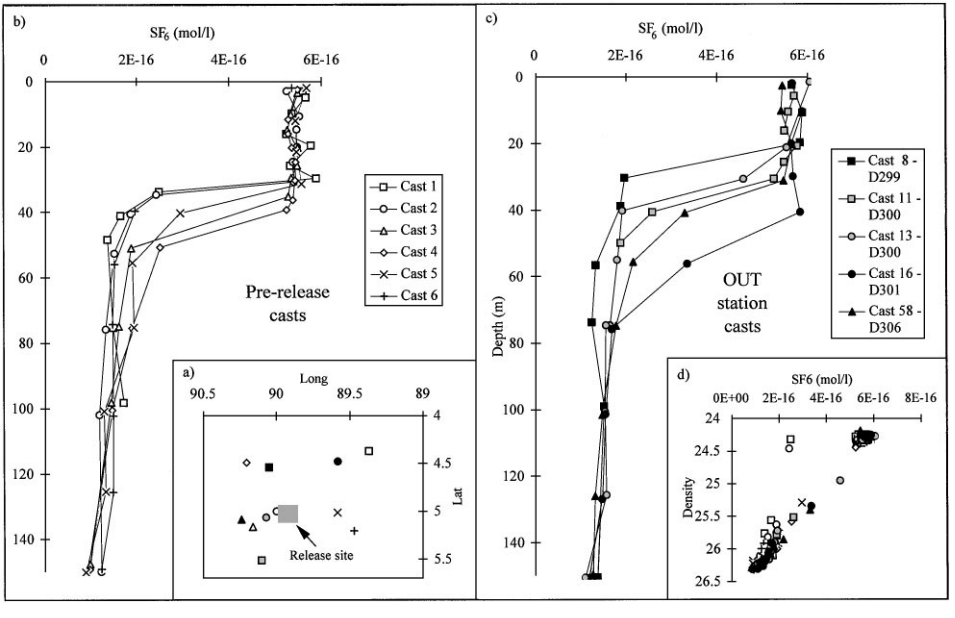


Fig. 1. (a) Positions of pre-release and OUT patch stations in the Equatorial South Pacific. The iron/ $SF_6$ release site is also shown. (b) Background $SF_6$ profiles at pre-release stations. (c) Background $SF_6$ profiles at OUT patch stations. (d) Background $SF_6$-Density relationship.

times the detection limit at 200 m. Variation in the upper water column structure was apparent, with Casts 1, 2 and 6 exhibiting a mixed-layer depth of 30 m, which apparently deepened to the west in Casts 3 and 4 (Fig. 1b). "OUT" station casts, collected after tracer release at sites outside the patch exhibited similar variability in mixed layer depth (Fig. 1c). $SF_6$ was elevated at 60 m in Cast 16, suggesting a shallower pycnocline gradient in this region. However, spatial trends were not apparent from high-resolution towyo data, and the apparent changes in mixed layer depth were attributable to internal wave displacements, which reached up to 20 m.

### 3.2. The surface $SF_6$ patch

Budgeting of the patch was obtained by correction for surface water advection in a Lagrangian frame of reference via the use of the central drogued GPS buoy (Stanton et al., this volume). For each sample, the ship's position was corrected by relating the position of the buoy to its starting position, with an additional correction for analytical delay and surface water pumping (total 4 min). For the purpose of this discussion the patch is defined as where $SF_6$ concentrations exceeded 5 times background ($>2.5$ fmol/l), with the patch centre defined as exceeding 50 times background ($>25$ fmol/l). The initial dispersal was estimated from two passes through the centre of the patch between JD298.8 and JD299.5, with subsequent images of the surface patch generated for each approximate 24 h period using a Kriging contour-fitting package (Fig. 2). Each image of the patch is described with reference to the mid-time point of the period during which measurements were made. Initially a butterfly sampling strategy was employed, but coverage on JD300 was clearly insufficient, and a grid pattern was adopted for the remainder of the experiment to resolve the patch. This improved the patch resolution as shown by comparison of the contour error estimates of 25–30% for the first and second periods and 4–7% for third and fourth. The patch centre (e.g., $>25$ fmol/l) at JD299.15 was rectangular and covered an area of approximately 66.5 $km^2$, with a total patch surface area of 214 $km^2$ resulting from horizontal dispersion. The patch remained relatively coherent after initial dispersion and mixing, with no evidence of filamenting or streaking as observed in previous tracer releases (Wanninkhof et al., 1993). As expected, "fringing" of the patch, where mixing at the edges resulted in a broadening of the low $SF_6$ margin and dilution of the patch centre, increased with time and was most evident by JD302.2. The patch centre decreased to 4.7 $km^2$ by JD302.2, with the total patch area only increasing in size by a further 30 $km^2$, despite compression in an eastwest direction (Fig. 2).

In principle, the distribution of the $SF_6$ could be used to calculate horizontal diffusivities. However, this was not one of the aims of the $SF_6$ release, and more accurate estimates were obtained from the GPS buoy data (Stanton et al., this volume). Slippage of the GPS buoy relative to the patch was apparent at an early stage after release. This can be seen from a comparison of the regions of high $SF_6$ ($>25$ fmol/l) uncorrected for surface water movement with the GPS buoy position (Fig. 3). The buoy and patch centre remained closely associated during the initial 24 h following release, but by JD301.15 the buoy was at the northwest edge of the patch centre, with complete separation by JD302.2. Both patch centre and buoy exhibited

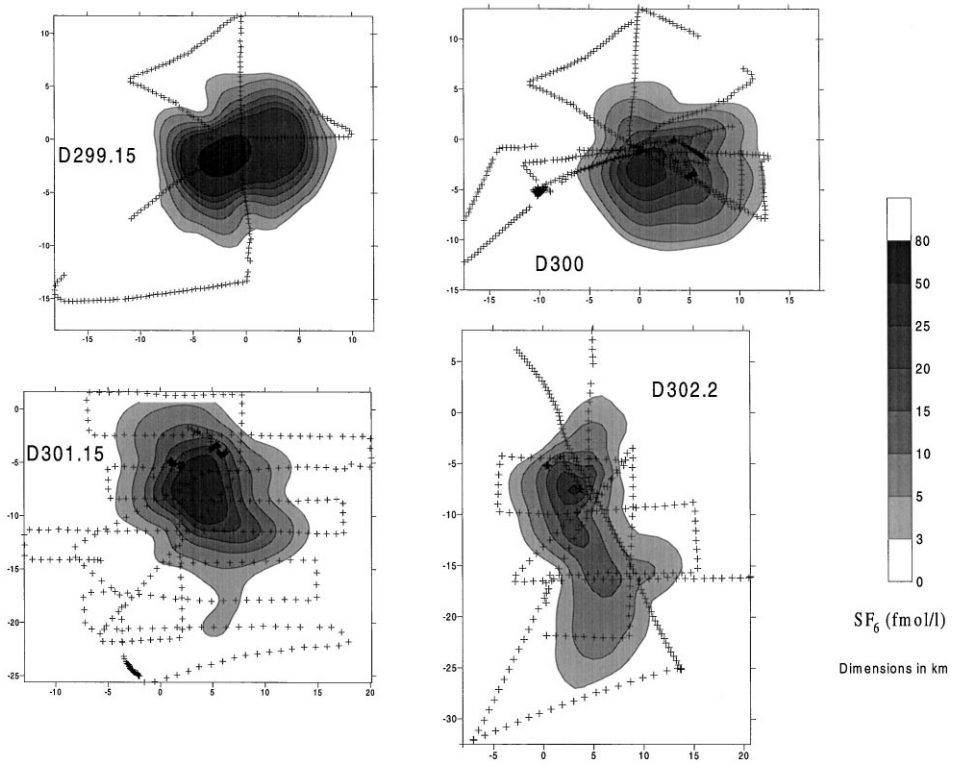


Fig. 2. The evolution of the $SF_6$ patch during the initial four days following release. All plots are corrected for GPS buoy position (0, 0) and are plotted in the same scale (km) to show the relative size and shape of the patch with time and the relative position to the buoy. The ships sampling position (+) is included to illustrate the coverage of the patch, and each plot is identified by its midpoint time in units of Julian Day. $SF_6$ concentrations are in fmol/l, and contouring of the patch was achieved using a Kriging data griding method in the SURFER Surface Mapping System (Version 5.2).

a slow anti-cyclonic oscillation generated by a large-scale wind-stress event (Stanton et al., this volume), with the GPS buoy displaced to the northwest. Undrogued buoys generally move at 1–2% of wind speed (Pingree, 1993), and so the relatively rapid "uncoupling" of the buoy and patch centre within 48 h of release was surprising. Displacement of the buoy resulted from a combination of wind-slippage, despite the drogue attachment, and strong near-surface shear generated by solar stratification. The slippage of the buoy and a corrective model are discussed further in Stanton et al. (this volume). Regardless of these observations, the GPS buoy provided essential information for mapping and budgeting of the patch by providing a Lagrangian drifter-referenced co-ordinate system. In practise it functioned as a locator for the centre of the patch, as observed in previous and subsequent $SF_6$ releases (Law et al., unpublished data). The influence of wind slippage and diurnal shear could be

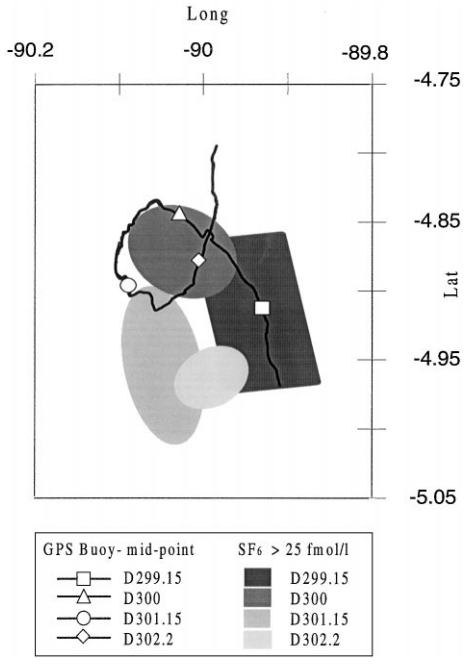


Fig. 3. Comparison of GPS Buoy position with $SF_6$ patch. The GPS Buoy track is shown by the solid line with the midpoint for each time period denoted by a symbol. The regions in which high $SF_6$ concentrations ($>25$ fmol/l) were obtained are shown uncorrected for surface water movement (e.g. not within a Lagrangian frame of reference), so that the relative positions of the GPS buoy and patch centre can be directly compared. The plot shows that by the second day after release the buoy was separated from the centre of the patch.

eliminated by modelling, but the lack of concurrence between buoy position and patch centre has implications for surface water flow studies and other tracer release experiments.

Good agreement was obtained for patch dimensions and total $SF_6$ (see Fig. 4) between the Kriging contouring approach and an Objective Analysis approach (Stanton et al., this volume). Release of 0.264 mol of $SF_6$ into an area of 64 $km^2$ with a mean mixed layer depth of 35 m would have increased the mean $SF_6$ concentration to 210 times background (118 fmol/l). This was, however, the highest concentration observed in the first 24 h period, with the patch centre exhibiting a mean concentration of only 65.5 fmol/l. Rapid lateral mixing and relatively sparse coverage resulted in the initial survey at JD299.15 accounting for only 0.171 mol $SF_6$ (see Fig. 2). As no sinks exist for $SF_6$ in surface waters, loss of $SF_6$ occurred through physical mechanisms. Diffusional loss across the air–sea interface was calculated from hourly windspeed data collected by two anemometers positioned on the ships bridge, with correction for ship's speed and bearing and height above sea level. Mean windspeed between release and JD302 was 5.6 m/s, with highest values of 8.5 m/s in the early

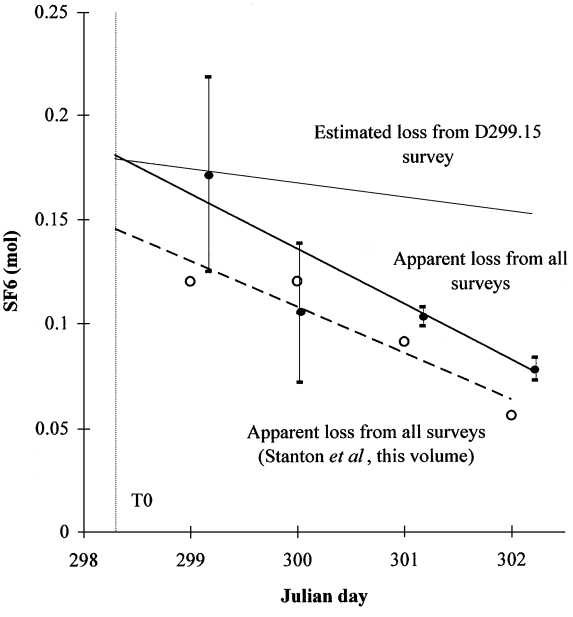


Fig. 4. Decline in total $SF_6$ in the patch based upon the Kriging data-griding method (black circles, solid line) and the objective analysis method (open circles, dashed line) of Stanton et al. (1998). Error estimates, based upon a nominal sphere of influence of each data point of 1.5 km, are included for each time period. The expected decline based upon loss via diffusion across the air–sea interface and thermocline from the JD299.15 survey is also shown. The tracer release time is shown as T0 (JD298.3).

hours of JD299 (Stanton et al., this volume) during the period when the initial assessment of the patch was made. Air–sea exchange accounted for a mean loss of 2.8% per day, as estimated from a wind-speed-transfer velocity relationship (Liss and Merlivat, 1986) and adjusted using a Schmidt no. of 934 at a surface temperature of 22.8°C (Wanninkhof, 1992). Diffusion across the thermocline was relatively insignificant (see below) and accounted for 0.42% per day, increasing the combined loss to 11.8% by JD302. Based upon the total at JD299.15 and a daily loss rate of 3.2% per day, the initial total SF6 was 0.178 mol at $T_0$ (JD298.3), which represents only 68.5% of the total saturated solution. As the $SF_6$ concentration was checked during the surface-water enrichment, it appears that a significant fraction of the $SF_6$ was lost to the atmosphere during the release into the prop wash via aeration and disturbance of the air–sea interface. Despite this loss, initial $SF_6$ concentrations were 120 times background levels and the patch remained detectable throughout the entire experiment.

The IN cast profiles generally exhibited constant $SF_6$ concentrations in the mixed layer, with a decline to background levels across the thermocline at 35 m (Fig. 5a). The $SF_6$ decrease in the surface waters of the first IN cast (Cast 9) on JD299 infers that vertical mixing was incomplete, or that a minor subduction event had occurred. The apparent deeper penetration of $SF_6$ in Cast 15 is a reflection of the change in the

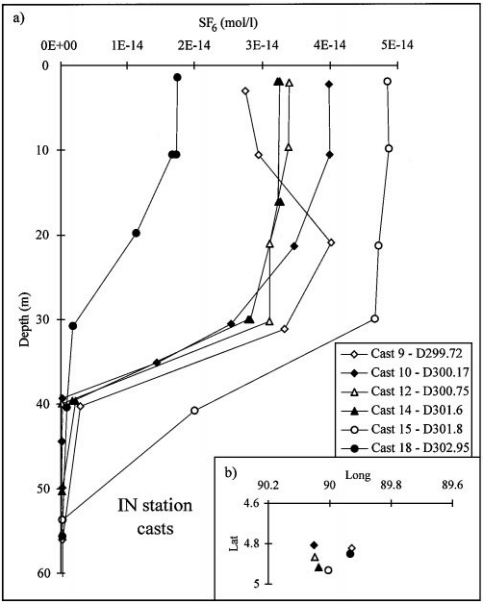


Fig. 5. (a) $SF_6$ profiles at the IN patch stations and (b) position of IN patch stations in the Equatorial South Pacific.

density distribution in the mixed layer, which deepened to 40 m (Fig. 5b), in response to internal wave displacements. $SF_6$ concentrations in Cast 18 on JD302 were significantly lower, as the patch had partially subducted to 20–30 m (see below). The discrete $SF_6$ data were used in conjunction with the discrete $pCO_2$ data to examine the potential for enhancing oceanic $CO_2$ uptake by iron fertilisation. In theory any increase in productivity in response to iron addition would result in a reduction in $pCO_2$ and so a decrease in $pCO_2/SF_6$ in the patch with time (Watson et al., 1991). A decrease in $fCO_2$ was observed initially after iron release, although this shift was generally most apparent in the $SF_6$ concentration range of 0–5 fmol/l, suggesting that corresponding iron concentrations were sufficient to relieve limitation (Watson et al., 1994). Turner et al. (1996) has used the $SF_6$ as a surrogate for the iron to identify an increase in DMSPp production following fertilisation of the surface waters. Spatial correlation was reported between the contoured $SF_6$ and chlorophyll data by JD300 (Martin et al., 1994), and photosynthetic activity exhibited a similar correlation within 24 h of release (Z. Kolber, pers. comm.). These observations confirm the limitation of productivity by iron in these waters, as well as demonstrating the capacity of the $SF_6$ tracer for evaluating ecosystem response in oceanic surface waters.

### 3.3. *Subduction of the $SF_6$ patch*

After sampling at an OUT station on JD301.92 (Cast 16) to the northeast (see Fig. 1a), considerable difficulty was experienced in re-locating the centre of the patch.

During the intervening period a low-salinity front moved across the region relatively rapidly from the southeast, resulting in subduction of the patch to 20–30 m during mid-late JD302 (Stanton et al., this volume). This can be seen in a series of $SF_6$ profiles obtained from late JD302 to JD303 (Fig. 6a). Cast 17 shows the patch centre (40 fmol/l) subducted to a depth of 30 m, whereas further northwest in Casts 19 and 24 the patch has only partially subducted (Fig. 6b). The lower $SF_6$ concentrations observed at depth at these two stations suggest that the trailing northwesterly edge of the surface patch was in the process of subduction. This was confirmed by Casts 18, 21 and 22 to the west, where the patch was still at the surface but $SF_6$ concentrations were $<20$ fmol/l. Fig. 7 shows that following subduction of most of the patch, the subducted patch centre and residual surface $SF_6$ maximum behaved relatively independently of each other, although it should be noted that these contour plots were uncorrected for movement of surface water as GPS buoy data were unavailable after JD304. The resultant surface $SF_6$ maximum, 4–5 times background levels, was displaced to the west relative to its position before the subduction event (see Fig. 2). By JD306.1–JD308.6 the surface patch had advected in a southwesterly direction and doubled in size. The subducted patch was located solely by the $SF_6$ signal and the patch centre remained relatively constant at $\sim 40$ fmol/l for the remainder of the experiment. This suggested that mixing with surrounding waters was minimal,

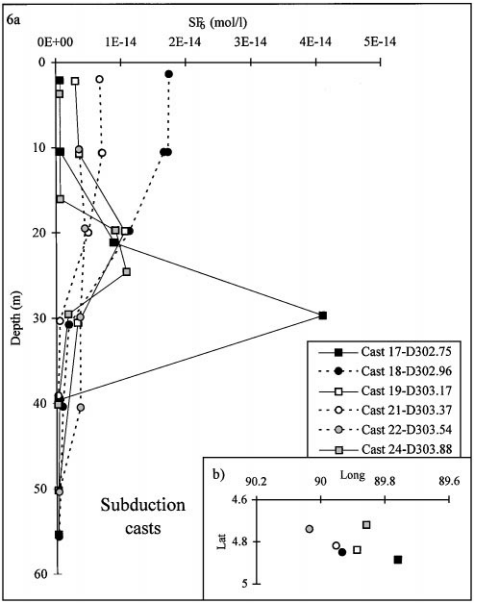


Fig. 6. (a) $SF_6$ profiles during the subduction event and (b) position of sampling stations during the patch subduction event. The profiles show that the centre of the patch was subducted in the southeast, whilst the trailing edge of the patch was in the process of subduction as evidenced by the lower $SF_6$ concentrations subducted and at the surface to the northwest.

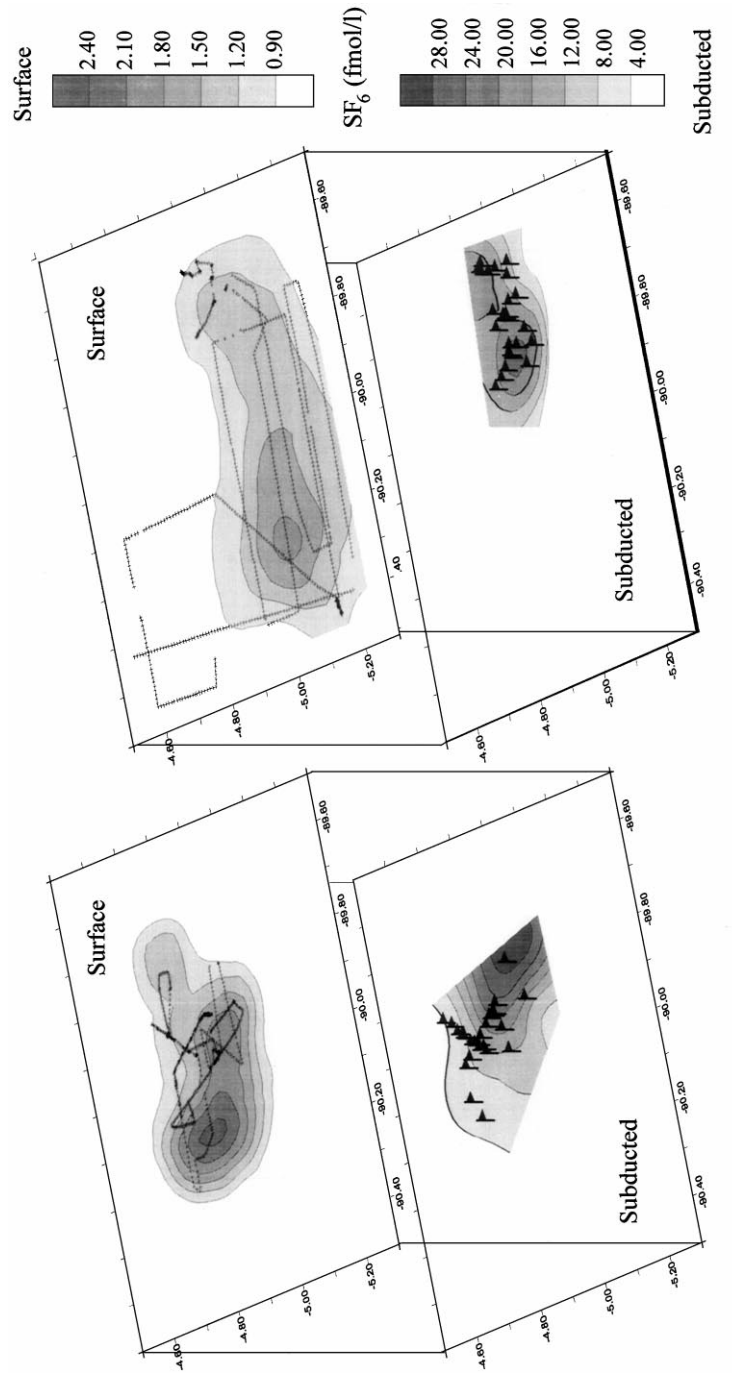


Fig. 7. Contour plots of the $SF_6$ patch following the subduction event with $SF_6$ concentration in fmol/l. The residual surface patch is shown in the upper plot with the ships sampling position shown as a solid line for both time periods. The subducted patch centre is shown in the lower plot, with the discrete sampling stations marked by pennants for both time periods. The plots are uncorrected for surface water movement as GPS Buoy data were unavailable. Contouring of the patch was achieved using a Kriging data griding method in the SURFER Surface Mapping System (Version 5.2).

although the consistency of the $SF_6$ signal was also due to isolation from the air–sea interface. After the initial displacement to the east upon subduction, the subducted patch centre remained relatively stationary in contrast to the surface patch (see Fig. 7), although coverage was limited by the discrete sampling mode. As the subducted patch remained in the euphotic zone the effects of iron fertilisation could still be studied once the location of the patch centre had been re-established, although light limitation at these depths probably led to a decline in the response (Johnson et al., 1996).

### 3.4. Vertical eddy diffusivity and new production

The vertical $SF_6$ profiles were utilised to determine the diapycnal diffusion rate ($K_z$) across the thermocline and into the overlying low salinity water following subduction of the patch. Eddy diffusion rates previously have been obtained directly using microstructure measurements (Lewis et al., 1986; Fielder et al., 1991, Carr et al., 1995), although as mixing is intermittent with short-term high dissipation events, these methods may result in an underestimate of diffusivity. Measurements of eddy diffusivity using the $SF_6$ tracer overcome this problem by providing an integrated rate over a relatively long time period (Ledwell et al., 1993). The $SF_6$ was originally released into surface waters with a relatively narrow density range, and so the resultant penetration of the tracer into adjacent waters with different density signals could be measured. To obtain vertical diffusivity rates, $SF_6$ was plotted against density for all of the detailed profiles, and then converted to density-corrected depth using the mean density profile following subduction (Fig. 8a). This transformation accounts for between cast variability in $SF_6$ resulting from vertical movement of density surfaces via internal waves. The profiles were interpolated to 2.5 m intervals, and grouped to obtain four average profiles spaced at approximately 24 h intervals starting from $T_0$, the time of subduction. The data were transformed into concentration versus depth plots and the interpolated $SF_6$ background concentration was subtracted from each profile (Fig. 8b). Variability in the magnitude of the $SF_6$ maximum resulted from the use of $SF_6$ profiles from stations which were not in the subducted patch centre. The 2nd moment was obtained from the following equation:

$$\int C(z - z_0)^2 \, \partial z / \int C \, \partial z$$

in which $C$ is the $SF_6$ concentration, $z_0$ is the depth of the peak maximum, and $z$ is the height above the peak maximum. The increase of the 2nd moment with time was then used to obtain $K_z$, as in previous estimates (Ledwell et al., 1993). The width was calculated separately for the upper and lower halves of the profile and a straight line fitted to the two relationships, with the slope of each line providing an estimate of $K_z$ (Fig. 8c).

The diffusion rates were obtained from the upper and lower surfaces of a "sandwiched" water body, and as such are unrepresentative of the upper ocean. In essence, structure developed within the mixed layer, with a weakly stratified slightly mixed subducted layer beneath a well-mixed wind-driven layer and overlying a strong pycnocline. As expected the vertical diffusion rates were higher on the upper surface, where the density gradient between the low salinity surface water and the

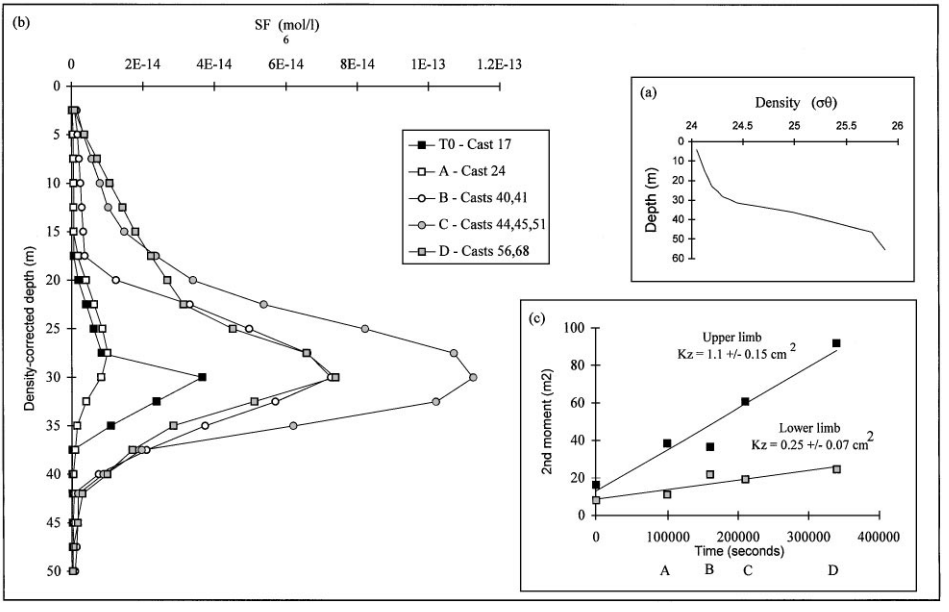


Fig. 8. (a) The mean density–depth profile for all casts following subduction of the patch. (b) Density-corrected depth profiles of $SF_6$ (mol/l) subdivided at ~24 h intervals. Variation in the size of the $SF_6$ maximum with time is a result of obtaining some casts near the edge of the patch. (c) The change of the second moment with time for the upper and lower limb of the $SF_6$ profiles plotted against time. The mean eddy diffusivity rate for each limb was calculated as twice the slope of the fitted lines.

tracer-labelled water was less steep than at the thermocline. Despite the fact that measurement of vertical diffusion rates was not the major goal of this $SF_6$ release and that a limited number of detailed profiles were obtained, the rate of 0.25 $cm^2\ s^{-1}$ is comparable with other estimates of diffusion using other techniques. The estimated $K_z$ was significantly higher than that of 0.09–0.1 $cm^2\ s^{-1}$ recorded at the base of the euphotic layer (58–80 m) between the equator and 5°S in the Pacific at 150°N (Carr et al., 1995). This difference is very likely due to the exclusion of significant intermittent mixing events in the microstructure measurements of the latter, as previously mentioned. A higher mean vertical diffusivity of 0.37 $cm^2\ s^{-1}$ was obtained in the permanent thermocline (100–400 m) from microstructure estimates over 2 week periods in the oligotrophic East Atlantic, with similar rates of 0.2–0.25 $cm^2\ s^{-1}$ obtained in the region of the seasonal thermocline at 40–50 m (Lewis et al., 1986). Both the source of energy giving rise to internal movement and the stratification of the water will influence rates of vertical mixing (Gargett, 1984). These vary from place to place, making direct comparison with previous estimates difficult. For example, vertical diffusivities of 0.11 and 0.2 $cm^2\ s^{-1}$ have been recorded in the permanent thermocline at 300 m in the sub-tropical North Atlantic (Ledwell et al., 1993) and at 440 m in the Sargasso Sea (Roether et al., 1971, Rooth and Ostlund, 1972), respectively.

Turbulence is the primary supply mechanism of new nutrients to the euphotic zone, and so the eddy diffusivity rates were utilised to determine nitrate supply across the pycnocline, and to estimate the contribution to new production. Nutrient profiles were transformed into density-corrected depth profiles and the gradient across the pycnocline estimated (Fig. 9). The flux was then calculated from Fickian diffusion theory using the equation:

$$F = -K_z \partial N/\partial z$$

where $K_z$ is the calculated vertical diffusivity, and $\partial N/\partial z$ the nutrient gradient across the thermocline at 35 m. The vertical flux of nitrate was estimated as 2.5 mmol $m^{-2} d^{-1}$, which would support a productivity of 0.2 g C $m^{-2} d^{-1}$, assuming a Redfield C:N ratio of 6.8. This flux is the same as that quoted by Lewis et al. (1986), but is considerably higher than the turbulent nitrate supply rate of 0.14 mmol $m^{-2} d^{-1}$ estimated for the Subtropical Atlantic Gyre (Lewis et al., 1986). A nitrate supply maximum of 1.9 mmol $m^{-2} d^{-1}$ was calculated for 5° either side of the equator in the Pacific along 150°W from a 3-D model (Carr et al., 1995), although this is lower than the mean rate estimated for the subducted patch due to the relatively more rapid transport in the eastern Pacific. This figure can be used to examine the *f*-ratio, defined as the ratio of new production to the sum of the new production; the premise of which is that the total flux of nitrate from the deep water must balance the total flux of particulate nitrogen out of the surface waters, assuming biomass remains constant. On comparison with the OUT station primary productivity rate of 15 μg C $l^{-1} d^{-1}$ (Martin et al., 1994) our estimate suggests an *f*-ratio of 0.4 for the subducted patch.

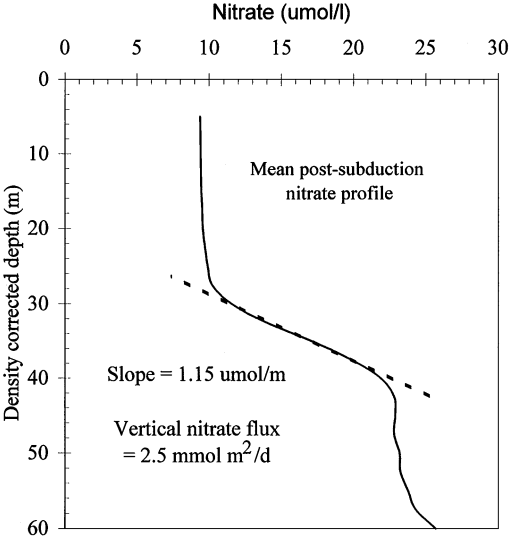


Fig. 9. Density-corrected depth profile of nitrate in the subducted patch. Nitrate diffusivity rates were calculated from the nitrate gradient at the thermocline.

This value is relatively high, exceeding that of 29% previously reported for the Eastern Tropical Pacific (Fiedler et al., 1991), which may be explained by the exclusion of the organic nitrogen component in our estimate.

## 4. Conclusions

The use of $SF_6$ in IRONEX provided a tool to determine the response of a number of variables to iron enrichment of the surface mixed layer. As such, a tracer release experiment of this kind overcame the limitations of conventional laboratory experiments and accommodated a mesoscale *in situ* experiment in which naturally occurring factors and influences were not excluded. This approach is not limited to manipulative experiments and has subsequently been extended to simple observational research in which the natural temporal changes within a water body are examined (Law et al., submitted; Martin et al., in press). The IRONEX1 data demonstrate that surface water movements can be accurately tracked using the tracer $SF_6$ in conjunction with buoys to provide a Lagrangian frame of reference. Vertical and lateral transport rates also may be derived using $SF_6$, thereby providing additional information which would benefit biological, biogeochemical and physical oceanographic research.

## Acknowledgements

The authors would like to thank the Captain, Officers and Crew of the RV *Columbus Iselin* and all members of the IRONEX group. In particular, we extend our thanks to Phil Nightingale, Kim Van Scoy and Sue Turner for assistance with $SF_6$ sampling and saturation, Jim Stockel for assistance with the GPS buoy data, Steve Fitzwater for the release apparatus, Gernot Friederich for the use of the MBARI CTD, and Sara Tanner for the nutrient data.

## References

Banse, K., 1990. Does iron really limit phytoplankton production in the offshore subarctic Pacific? Limnology and Oceanography 35(3), 772–775.

Carr, M.E., Lewis, M.R., Kelley, D., 1995. A physical estimate of new production in the equatorial Pacific along 150°W. Limnology and Oceanography 40(1), 138–147.

Fielder, P.C., Philbrick, V., Chavez, F.P., 1991. Oceanic upwelling and productivity in the eastern tropical Pacific. Limnology and Oceanography 36, 1834–1850.

Fitzwater, S., Coale, K., Blain, S., Coley, T., Hunter, C., Johnson, K., 1994. The design and implementation of a mesoscale iron enrichment experiment in the equatorial Pacific. EOS. 75(3), 150.

Gargett, A.E., 1984. Vertical eddy diffusivity in the ocean interior. Journal of Marine Research 42(2), 359–393.

Johnson, K.S., Gordon, R.M., Coale, K.H., Elrod, V.A., 1996. Iron in IronEx 1, IronEx 2 and the Galapagos PlumEx. EOS, Transactions of the American Geophysical Union 76(3), 154.

Ko, M.K.W., Sze, N.D., Wang, W.-C., Shia, G., Goldman, A., Murcray, D.G., Rinsland, C.P., 1993. Atmospheric Sulfur hexafluoride: sources, sinks and greenhouse warming. Journal of Geophysical Research 98(D6), 10 499–10 507.

Law, C.S., Watson, A.J., Liddicoat, M.I., 1994. Automated vacuum analysis of Sulphur hexafluoride in seawater; derivation of the atmospheric trend (1970–1993) and potential as a transient tracer. Marine Chemistry 48, 57–69.

Law, C.S., Liddicoat, M.I., Martin, A.P., Richards, K.J., Woodward, E.M.S., A Langrangian $SF_6$ tracer study of an anti-cyclonic eddy in the North Atlantic: patch evolution, vertical mixing and nitrate supply to the mixed layer. Deep-Sea Research, submitted.

Ledwell, J.R., Watson, A.J., Law, C.S., 1993. Evidence for slow mixing across the pycnocline from an open-ocean tracer-release experiment. Nature 364, 701–703.

Lewis, M.R., Harrison, W.G., Oakey, N.S., Herbert, D., Platt, T., 1986. Vertical nitrate fluxes in the oligotrophic ocean. Science 234, 870–873.

Liss, P.S., Merlivat, L., 1986. Air-sea gas exchange rates: Introduction and sysnthesis. In: Buat-Menard, P. (Ed.), The Role of Air-Sea Exchange in geochemical Cycling. Reidal, MA, pp. 113–129.

Maiss, M., Levin, I., 1994. Global increase of $SF_6$ observed in the atmosphere. Geophysical Research Letters 21(7), 569–572.

Maiss, M., Steele, P., Francey, L.P., Fraser, P.J., Langenfelds, R.L., Trivett, N.B.A., Levin, I., 1996. Sulfur hexafluoride-a powerful new tracer. Atmospheric Environment 30, 1621–1629.

Martin, J.H., Coale, K., Johnson, K., Fitzwater, S., Gordon, M., Tanner, S., Hunter, C., Elrod, V., Nowicki, J., Coley, T., Barber, R., Lindley, S., Watson, A., Van scoy, K., Law, C.S., Liddicoat, M., Ling, R., Stanton, T., Stockel, J., Collins, C., Anderson, A., Bidigare, R., Ondrusek, M., Latasa, M., Millero, F.J., Lee, E., Yao, W., Zhang, J.Z., Friederich, G., Sakamoto, C., Chavez, F., Buck, K., Kolber, Z., Greene, R., Falkowski, P., Chisholm, S.W., Hoge, F., Swift, R., Yungel, J., Turner, S., Nightingale, P., Hatton, A., Liss, P., Tindale, N., 1994. Testing the iron hypothesis in ecosystems of the equatorial Pacific Ocean. Nature 371, 123–129.

Martin, J.H., Fitzwater, S.E., 1988. Iron deficiency limits phytoplankton growth in the north-east Pacific subarctic. Nature 331, 341–343.

Martin, J.H., Fitzwater, S.E., Gordon, R.M., 1990. Iron deficiency limits phytoplankton growth in Antarctic waters. Global Biogeochemical Cycles 4(1), 5–12.

Martin, A.P., Richards, K.J., Law, C.S., Liddicoat, M.I., Horizontal dispersion in an anti-cyclonic eddy. Deep-Sea Research II, in press.

Pingree, R.D., 1993. Flow of surface waters to the west of the British Isles and in the Bay of Biscay. Deep-Sea Research II 40, 369–388.

Roether, W., Munnich, O., Ostlund, H.G., 1971. Tritium profile at the North Pacific. 1969. Geosecs Intercalibration Station. Journal of Geophysical Research 75(36), 7672–7675.

Rooth, C.G., Ostlund, H.G., 1972. Penetration of tritium into the Atlantic thermocline. Deep-Sea Research 19, 481–492.

Stanton, T., Law, C.S., Watson, A.J., 1998. Physical evolution of the IRONEX-1 open ocean tracer patch. Deep-Sea Research II 45, 947–975.

Smart, P.L., Laidlow, I.M.S., 1977. An evaluation of some fluorescent dyes for water tracing. Water Resources Research 13, 15–33.

Turner, S.M., Nightingale, P.D., Spokes, L.J., Liddicoat, M.I., Liss, P.S., 1996. Increased dimethyl sulphide concentrations in seawater from in situ iron enrichment. Nature 383, 513–517.

Upstill-Goddard, R.C., Watson, A.J., Liddicoat, M.I., Wood, J., 1991. Sulphur hexafluoride and Helium-3 as seawater tracers deployment techniques and continuous underway analysis of SF6 by purge and cryotrap ECGC. Analytica Chimica Acta 249, 555–562.

Wanninkhof, R., 1992. Relationship between wind speed and gas exchange over the ocean. Journal of Geophysical Research 97(C5), 7373–7382.

Wanninkhof, R., Asher, W., Weppernig, R., Chen, H., Schlosser, P., Langdon, C., Sambrotto, R., 1993. Gas transfer experiment on Georges Bank using two volatile deliberate tracers. Journal of Geophysical Research 98(C11), 20 237–20 248.

Wanninkhof, R., Ledwell, J.R., Watson, A.J., 1991. Analysis of sulphur hexafluoride in seawater. Journal of Geophysical Research 96(C5), 8733–8740.

Watson, A.J., Law, C.S., Vanscoy, K., Millero, F.J., Yao, W., Friederich, G.E., Liddicoat, M.I., Wanninkhof, R.H., Barber, R.T., Coale, K.H., 1994. Minimal effect of iron fertilization on sea-surface carbon dioxide concentrations. Nature 371, 143–145.

Watson, A.J., Liddicoat, M.I., 1985. Recent history of atmospheric trace gas concentrations deduced from measurements in the deep sea: application to sulphur hexafluoride and carbon tetrachloride. Atmospheric Environment 19, 1477–1484.

Watson, A.J., Upstill-Goddard, R.C., Liss, P.S., 1991. Air-sea gas exchange in rough and stormy seas measured by a dual-tracer technique. Nature 349, 145–147.